ACADEMIA ROMÂNĂ
Revue Roumaine de Chimie
http://web.icf.ro/rrch/

Rev. Roum. Chim.,
2016, *61*(6-7), 565-573

Dedicated to Professor Dumitru Oancea
on the occasion on his 75th anniversary

UPON THERMAL CHARACTERIZATION OF A MAGNETIC COMPOSITE IN RELATION WITH THE POLY(SUCCINIMIDE)-b-POLY(ETHYLENE GLYCOL) SHELL PROPERTIES

Nita TUDORACHI,[a] Waldemar KNAUER,[b] Aurica P. CHIRIAC,[a*] Loredana E. NITA,[a]
Iordana NEAMTU[a] and Manuela T. NISTOR[a]

[a] "Petru Poni" Institute of Macromolecular Chemistry 41-A Grigore Ghica Voda Alley, 700487 Iaşi, Roumania
[b] NETZSCH-Gerätebau GmbH, BU Analyzing & Testing

Received November 11, 2015

In the paper the deep thermal characterization of the core-shell magnetic composite in relation with the properties of the shell formed from poly(succinimide)-b-poly(ethylene glycol) (PSI-b-PEG), respectively the molecular weight of poly(ethylene glycol), is presented. The study confirms the dependence of the thermal stability, for both the synthesized block copolymers and the prepared magnetic composites, on the molecular weight of PEG. Also, the influence of the Fe atoms presence was concretized in autocatalytic effect for thermal degradation. Information resulted from the thermal analysis are sustained by the contact angle values of the block copolymer surface as well by the morphological aspects of the block copolymer films.

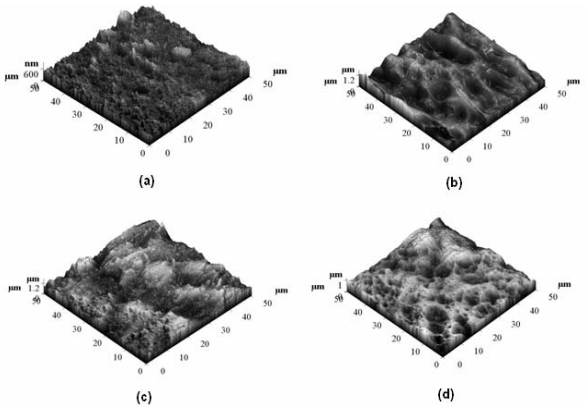

INTRODUCTION

Interest in the use of synthetic structures for biomedical applications is growing. This in a context where they can ensure biocompatibility and/or biodegradability and versatility required for use. Polymeric structures also offer significant advantages as well as carrier platforms as long as they allow for tailoring the properties to meet the specific intended need. Other advantages of polymeric matrices include ease of surface modification, encapsulation efficiency of the payload, payload protection, large area-to-volume, slow or fast polymer degradation and stimuli-responsive polymer erosion for temporal control over the release.[1] From this point of view poly(succinimide) (PSI) and poly(ethylene glycol) (PEG) are products which confirmed their usefulness and applicability in the biomedical field.[2 - 11] In one of our previous papers the

* Corresponding author: achiriac1@yahoo.com

possibility to prepare the block copolymer between PSI and PEG (with different molecular weights of about 2000, 4000, 10000 or 20000) is presented.[12] The block copolymer was characterized from the viewpoint of its structure and thermal stability.

Taking into account that magnetic particles with suitable surface characteristics have high potential for use in a lot of *in vitro* and *in vivo* applications, we also presented the *in situ* preparation of a core-shell magnetic composite with magnetite core and shell composed from the poly(succinimide)-b-poly(ethylene glycol) copolymer.[13] The average particle size of the synthesized magnetic microspheres was in the range of 6.5–8.8 μm with a magnetite content of around 11%. The saturation magnetization of the microspheres was found 26.8 emu/g, the magnetic microspheres being characterized by superparamagnetic properties. The particles have combined properties of high magnetic saturation and biocompatibility and interactive functions at the surface owing to the block copolymer shell. The surface of the magnetic particles has also the possibility for further functionalization or attachment of various bioactive compounds after hydrolysis of the succinimide cycle and the resulting carboxylic group.[14]

In this investigation the deep thermal characterization of the core-shell magnetic composite in relation with the properties of the shell formed from poly(succinimide)-b-poly(ethylene glycol)(PSI-b-PEG), respectively the molecular weight of poly(ethylene glycol), is presented. A relationship was established between the thermal behavior of PSI-b-PEG and the contact angle measurements of the block copolymer and also the surface topology and smoothness of films of the polymeric shell.

RESULTS AND DISCUSSION

As it is well known PEG is the most commonly applied non-ionic hydrophilic polymer with stealth behavior. At the same time PEG reduces the tendency of particles to aggregate by steric stabilization, and thus producing formulations with increased stability during storage and application. [15] Based on the studies of Kabanov *et al.*,[16-18] who was the first that proposed the use of PEG as a hydrophilic part of linear block copolymers for micellization, we tested the PSI-b-PEG as shell for preparation of a magnetic composite. In Table 1 are presented the investigated copolymers and magnetic composites.

The purpose was to have an amphiphilic shell, which exhibits enhanced surface functionality and possibility to control the size and shape of the micelles that include the magnetic compound, through the molecular weight of both compounds. In the present study there are underlined the differences in thermal characteristics of the magnetic composite generated by the differences in the molecular weight of PEG as component in the block copolymer shell, data which are sustained through the differences in contact angle of the PSI-b-PEG film as well by the polymeric film morphology. TG and DTG curves for the samples taken into study and recorded at $10^{o}C \cdot min^{-1}$ heating rate are illustrated in Fig. 1a - d.

Table 1

The main components of the copolymers and magnetic composites

Sample	Code sample	PSI (g)	PEG (g)	Magnetite (g)
PSI-b-PEG_{2000}	P2	2	1	-
PSI-b-PEG_{2000} /magnetite	MC2	2	1	0.33
PSI-b-PEG_{4000}	P4	2	1	-
PSI-b-PEG_{4000} /magnetite	MC4	2	1	0.33
PSI-b-PEG_{10000}	P10	2	1	-
PSI-b-PEG_{10000} /magnetite	MC10	2	1	0.33
PSI-b-PEG_{20000}	P20	2	1	-
PSI-b-PEG_{20000} /magnetite	MC20	2	1	0.33

PSI (Mn=15551); PEG_{2000} (Mn=2000); PEG_{4000} (Mn=4000); PEG_{10000} (Mn=10000); PEG_{20000} (Mn-20000).

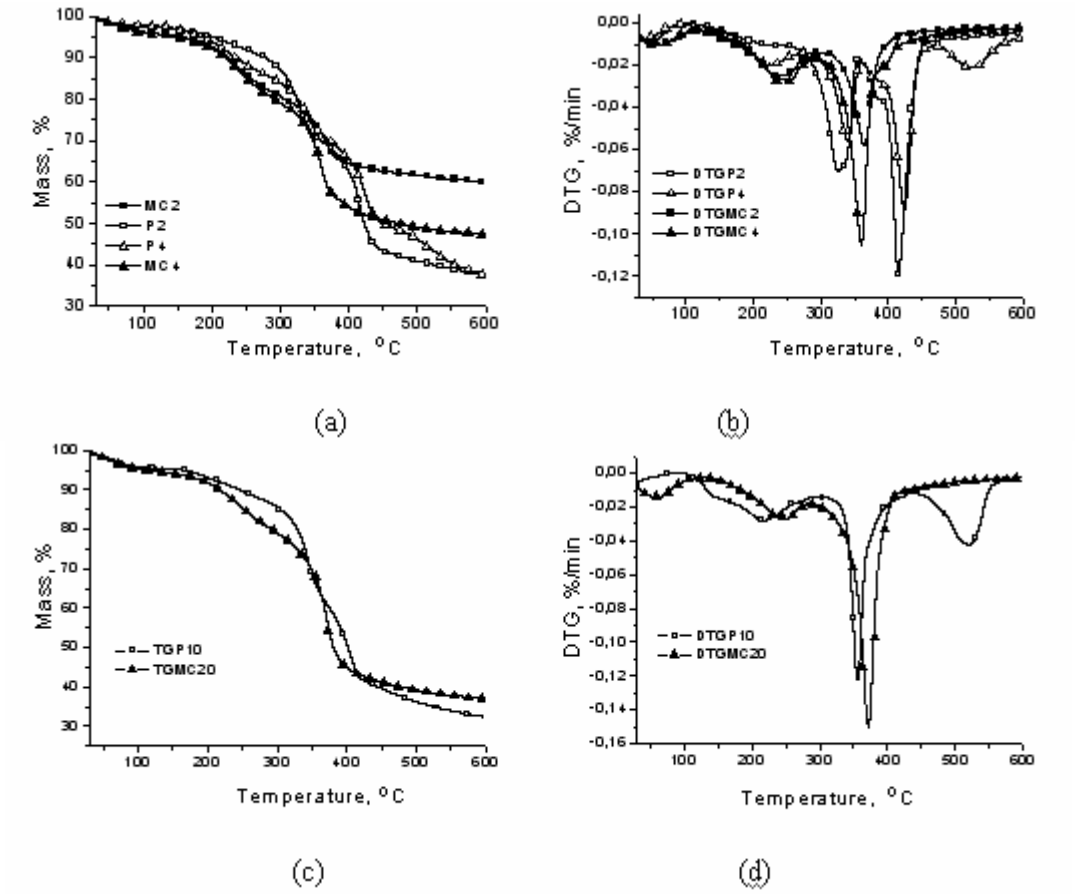

Fig. 1 – TG and DTG curves of samples taken into study: TG for P2, P4, MC2, MC4 **(a)**; DTG for P2, P4, MC2, MC4 **(b)**; TG for P10, MC20 **(c)**; DTG for P10, MC20 **(d)**.

In general, **thermal decomposition processes** occur in three stages of decay, except for copolymer P4 where thermal decomposition takes place in four stages. In the first stage of thermal degradation, T_{onset} varies between 35°C and 115°C and the mass losses are due mainly to adsorbed water at the copolymers and composites surface and water connected by hydrogen bonding into PEG segment. P2 and P4 samples recorded mass losses of about 63 wt %, while the correspondingly nanocomposite MC2, MC4 of 40 wt%, respectively 53 wt% is mainly due to copolymer degradation. The thermal stability of polymers and nanocomposites can be analyzed in relation with T10 and T20 values, temperatures occurring mass loss of 10 and 20 wt% respectively. For P2 sample the weight loss of 10 wt% and of 20 wt% occurs at temperatures of 277°C and respectively 324°C, while for corresponding nanocomposite (MC2) at 223°C and 307°C. On the other hand, in case of P4 copolymer these losses are recorded at 234°C and 325°C, whereas its nanocomposite MC4 presents these registrations at 219°C and 291°C respectively. It can be concluded that higher molecular weight for PEG corresponds to relative decreased thermal stability.

At the same time, lower thermal stability of nanocomposites compared with copolymers can be justified by the iron atoms presence (Fe_3O_4), who plays the role of catalyst for decomposition of the macromolecular chains and breaking of C-C, C-N or C-O chemical bonds. The magnetite content from PSI-b-PEG/magnetite composite was also determined by thermogravimetry, considering the residue at 600°C for magnetic nanocomposite and PSI-b-PEG copolymer:

$$(MC2)60.00 - 37.58 = 22.42\ wt\%\ magnetite$$
$$(MC4)47.17 - 37.68 = 9.49\ wt\%\ magnetite$$

Data agree with the reaction conditions, respectively 10 % magnetite were considered optimum for manifesting the superparamagnetic properties. At the same time higher content of magnetite corresponds to polymeric shell with PEG having reduced molecular weight, which means a better capacity of micellization for this block copolymer.

Kinetic investigations made for samples taken into consideration were conducted at three heating rates (5, 10, 20°C·min^{-1}) in the range temperature between 150 to 500°C, where weight loss determined by thermal decomposition was significant (47-57 wt %). The recorded experimental data were processed in order to determine the kinetic parameters of thermal degradation. Because the analyzed samples present approximately the same behavior resulted from kinetic analysis (made using "Thermokinetics 3"software, Netzsch [19]), in this study only analysis for P20 copolymer and MC20 nanocomposite, is mentioned. At the beginning the isoconversional method of FR was used to calculate the variation of activation energy (Ea) *versus* the conversion degree (α). Taking into account the shape of DTG curves (where at least three peaks were observed) and the variation of the activation energy of the thermal decomposition *versus* conversion degree (Fig. 2 a, b), it can be considered that the thermal degradation process is a complex process occurring in multiple steps.

Based on TG data recorded at three different heating rates and using the multivariate non-linear regression method, the software solved the differential equations contained in it and determined the kinetic and statistic parameters for the thermal degradation processes. [19,20]

Calculations were done on the range between 0.2 and 0.8 for the conversion degree (α). The next conversion functions were considered:

- Avrami–Erofeev reaction model:

$$An: f(\alpha) = n(1-\alpha)[-\ln(1-\alpha)]^{n-1/n}$$

where *n* is a constant parameter, and

- n_{th} reaction order model,

$$Fn: f(\alpha) = (1-\alpha)^n$$

where *n* is the reaction order.

The two- and three-step reaction models A-1 → B-2 → C and A-1 → B-2 → C-3 → D with consecutive reactions were taken into account with the next kinetic models: d:f; An, Fn and t:f,f; Fn, Fn, Fn for P20 sample; d:f; Fn, Fn and t:f, f; Fn, An, Fn for the MC20 magnetic nanocomposite, where: A, B, C, D are solid products, d, f – represent the thermal processes in two stages in which the individual steps are linked as consecutive reactions of n–th order and 1, 2, 3 symbolize the mechanism steps.

By using the conversion functions and mechanisms represented above, the software calculates the kinetic and statistics parameters and after that the thermal degradation processes are occurring. The obtained values are listed in Table 2.

In general, lower values of the activation energy are standing in case of magnetic nano-composites, possibly owing to the catalytic effect generated by Fe atoms from magnetite. The reaction order values lower than 1 suggest that thermal degradation occurs mainly by cleavage of the macromolecular chains in small molecules, followed by a probable cyclization, while the values higher than 1 imply that outside the small molecules short fragments of polymeric chains also appear.[21] The models were chosen taking into account the maximum value of the correlation coefficient and also the base of minimum differences between experimental data and the calculated data. The overlapping between TG experimental curves and those calculated with kinetic parameters from Table 2 is given in Fig. 3. It can be observed a very good correlation between the data for both samples, all having the correlation coefficient higher than 0.99. This fact shows that the chosen kinetic models describe well the thermal degradation reactions.

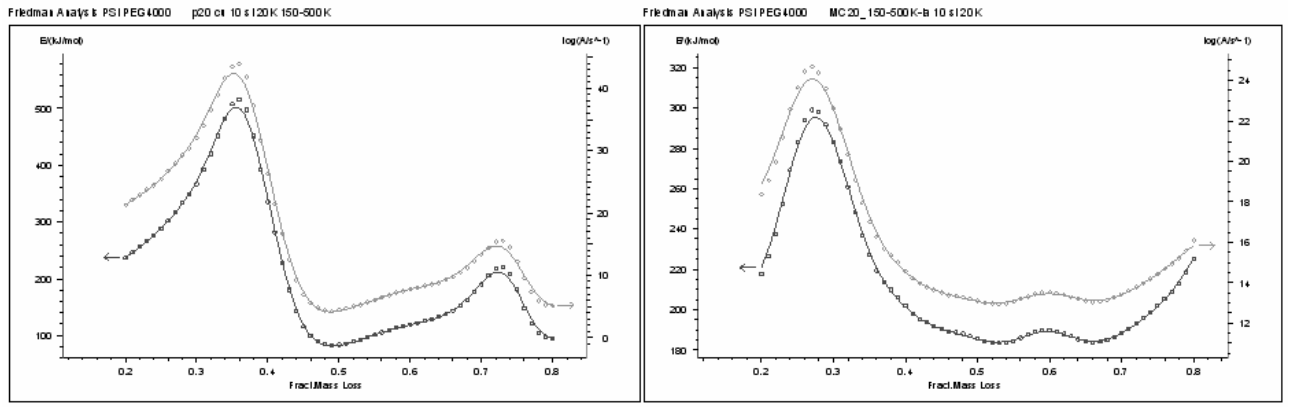

(a) (b)

Fig. 2 – Variation *E*a and log *A versus* conversion degree for P20 (a) and respectively MC20 (b).

Table 2

The kinetic parameters and statistics, determined after non-linear regression method for the most probable mechanism of thermal degradation process, by applying a three-step kinetic model with consecutive reactions on the temperature interval between 150-500 ^{o}C

Parameters[a]	Sample			
	P20		MC20	
	Mechanism scheme			
	A-1 → B-2 → C-3 → D	A-1 → B-2 → C	A-1 → B-2 → C-3 → D	A-1 → B-2 → C
	Kinetic model type			
	t:f,f; Fn,Fn,Fn	d:f; An,Fn	t:f,f; Fn,An,Fn	d:f; Fn,Fn
E_1 (kJ·mol^{-1})	165	226	120	115
log A_1 (s^{-1})	15.833	21.258	10.610	9.997
Dimension d_1	-	0.31	-	-
React ord n_1	2.82	-	2.86	2.99
E_2 (kJ·mol^{-1})	186	203	106	190
log A_2 (s^{-1})	13.421	14.830	23.02	13.845
React ord n_2	2.88	2.99	-	2.35
Dimension d_2	-	-	0.814	-
E_3 (kJ·mol^{-1})	110	-	157	-
log A_3 (s^{-1})	22.717	-	11.057	-
React ord n_3	0.98	-	2.07	-
FollReact 1	0.274	0.289	0.145	0.308
FollReact 2	0.405	-	0.140	-
Mass loss 5Kmin^{-1}, %	52.44	52.44	57.50	57.50
Mass loss 10 Kmin^{-1}, %	48.91	48.91	56.61	56.61
Mass loss 20 Kmin^{-1}, %	47.71	47.71	55.97	55.97
Correln. coeff.	0.989212	**0.990670**	0.997994	**0.998586**

E_1, E_2, E_3 – activation energy for each step, log (A_1, A_2, A_3) - pre-exponential factor for each step. n_1, n_2, n_3, – reaction order, d_1, d_2 - dimension coefficients according with Avrami-Erofeev model, FollReact 1, FollReact 2-share of reaction step 1 (A→B), step 2 (B→C), step 3 (C→D) in the total mass loss.

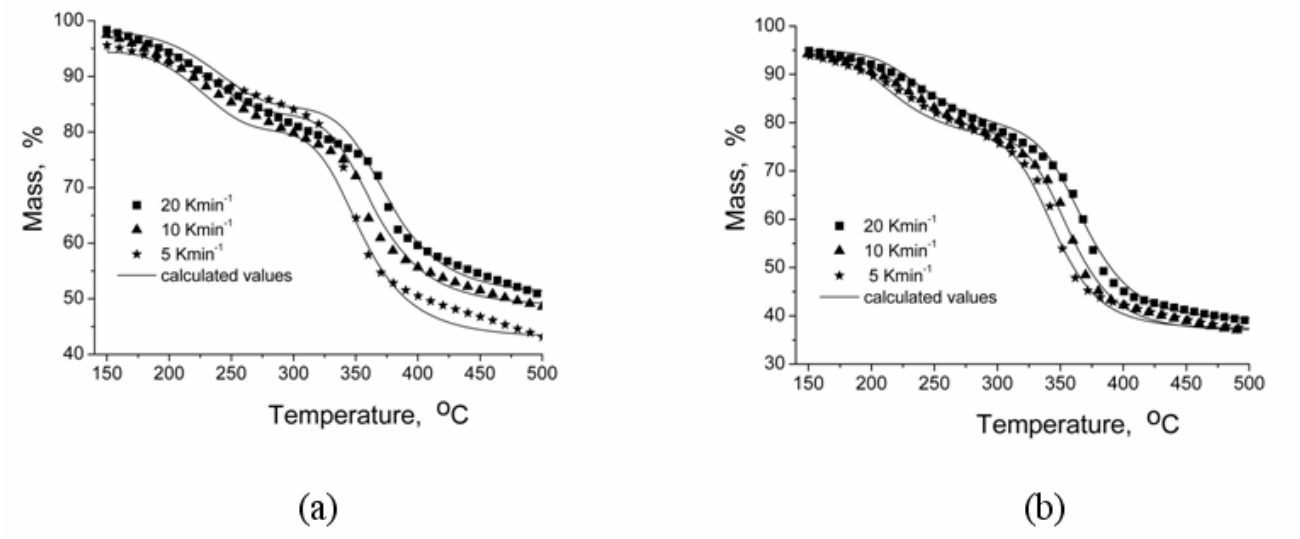

Fig. 3 – The regenerated TG curves of P20 (a) and MC 20 (b). The symbols represent the experimental values at three different heating rates and the straight lines represent the calculated values.

The contact angle measurements for the films made from PSI-b-PEG polymeric shell (presented in Experimental section, Table 3) agree with the literature data in the field. [22-24] Thus, PSI-b-PEG films are characterized by a good wettability as long as PEG is strongly hydrophilic as well as PAS

(PSI is the precursor of PAS). Anyway PSI film presents a moderate wettability (with a contact angle of about 54 which attests its less hydrophilic surface than that of PEG) and PSI block copolymer with PEG is generating films with a variable contact angle which are also in interdependence with the molecular weight of PEG. The measured contact angle decreases as the molecular mass of PEG increases. This aspect is entirely justified taking into account that the ratio between PSI and PEG decreases as the molecular weight of PEG increases and the dominant in determining the contact angle is generated by the hydrophilic compound that shows a contact angle of 25°.

Morphological information concerning the studied samples sustain also the data resulted from thermal analysis as well those concerning the determined contact angles. The structural and compositional characteristics of the block copolymers surfaces are evidenced and differences between the polymeric shells in relation with their composition are proved. Fig. 4,a-d presents the direct high-resolution visualization of the film surfaces made from P2, P4, P10 and P20 block copolymers.

The compositional mapping corresponding to block copolymers in relation with the molecular weight of PEG is evident. Thus, for P2 a structural heterogeneity is the common feature, revealing the homogeneity of the molecular mass for both polymeric components PSI (~ 16000) and PEG (20000). At the same time a complex morphology with existing ordered and smooth domains alternates, with partially ordered irregularities or mesomorphic form, which can also be characterized by phase imaging.

In case of these block copolymers the phase contrast, which is very sensitive to the differences in material properties, respectively differences of the molecular weight between PSI and PEG, is also present (Fig. 4 c and d). Thus, the sample is populated with edge-on zones specific to compositional imaging of multicomponent polymer structure. Consequently, the brighter areas in the phase image (corresponding deeper areas in topographic image) are attributed to domains generated by the PSI with lower molecular weight.

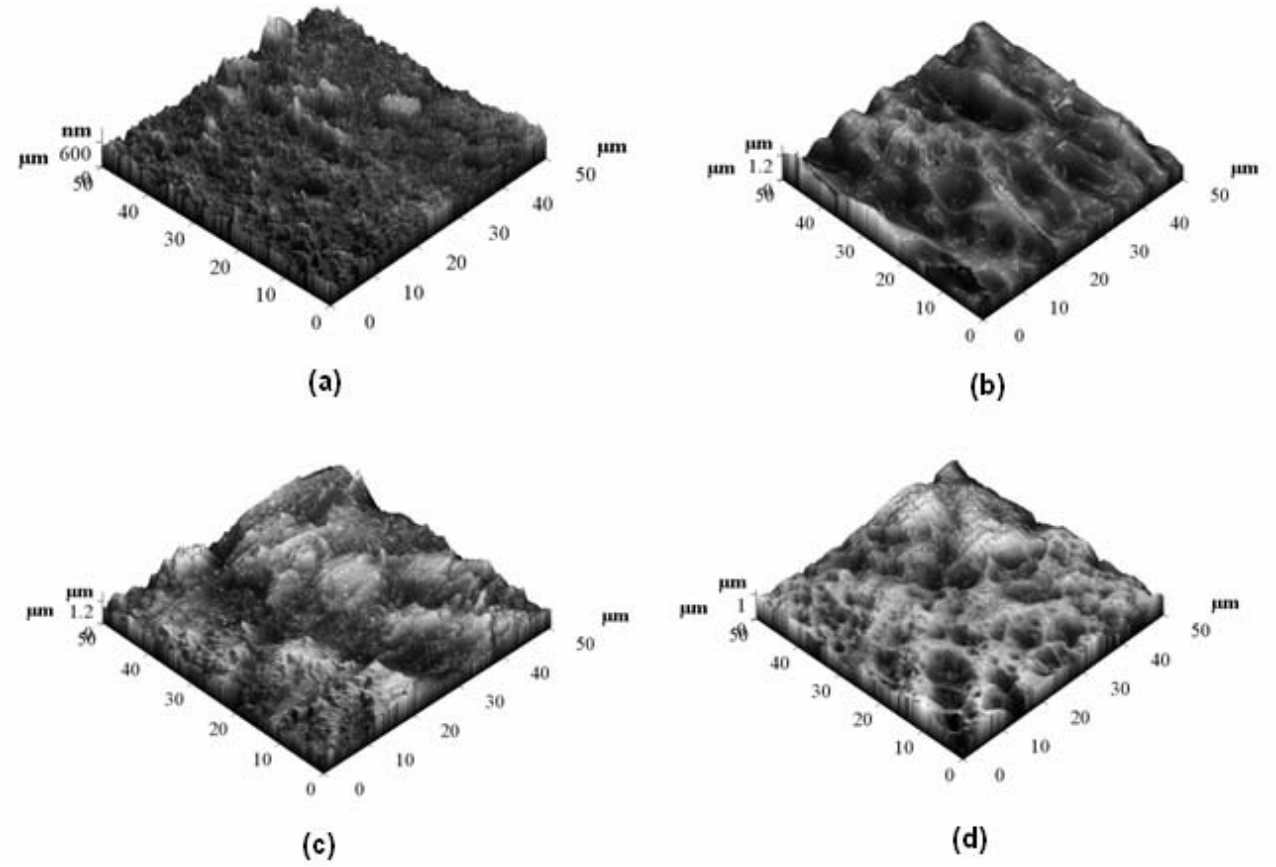

Fig. 4 – AFM three-dimensional images of films from P20 (a), P 10 (b), P4 (c) and P2 (d) block copolymers.

EXPERIMENTAL

Materials and magnetic composite synthesis procedure

Dodecane (Fluka Chemika, purity > 90%), DMF (Fluka Analytical, purity > 98%) l-aspartic acid (Fluka BioChemika), o-phosphoric acid (analytical reagent of 85%, Chemical Co. Roumania), manganese (II) acetate (Sigma Aldrich, purity 98%), were used as received. Poly(ethylene glycol) (PEG) (with molecular weights of 2000, 4000, 10000, and 20000) was purchased from Fluka Germany and used without further purification.

The procedure for polymeric shell synthesis and magnetic composite preparation were previously in detail presented [12,13], but shortly these are the steps:

The synthesis of the magnetite particles has been previously performed by a conventional coprecipitation method between a solution containing $FeCl_2$ (0.033M) and $FeCl_3$ (0.067M) which was poured into a base solution of NaOH (200mM) under stirring at 60°C. The ferrofluid suspension of Fe_3O_4 was cooled at room temperature. The black solid was settled over a magnet, leaving a clear supernatant liquid that was decanted. The black solid of Fe_3O_4 was washed several times with acetone and methanol, and the precipitates were isolated from the solvent by magnetic decantation. This washing–decantation procedure was repeated three times.

In the first step, the precursor poly(succinimide) (PSI) was synthesized by polycondensation of l-aspartic acid in dodecane, at 180°C, for 6 h, using o-phosphoric acid as catalyst. In a typical experiment, the reaction is carried out in a 250mL three necked round-bottom flask equipped with mechanical stirrer, a Dean–Stark trap fitted on water condenser, with thermometer in the vapor circuit, and heated in a thermo-regulated oil bath. The average molecular weight of PSI determined by Gel Permeation Chromatography (GPC), in dimethylformamide (DMF) as solvent, was Mn=15551 and polydispersity index 1.731.

In the second step, the preparation of the magnetic composite was carried out. The same equipment was charged with 15mL DMF as reaction medium, 2 g of PSI, 1 g PEG (with the molecular weight specific for each sample, grounded to fine powder form in a porcelain mortar), and 11.78 g stabilized ferrofluid with the concentration of 2.8% in ferrite. The ratio between the magnetite and the polymeric components was established to have finally a content of at least 11% magnetite in the magnetic composite (data established from the magnetic composite thermal decomposition analysis, which is presented before). The weight ratio of magnetite plays an important role in controlling the magnetite content into the final particles composite as well as composites response as superparamagnetic hybrids.

The mixture is heated at 138°C and 0.045 g of manganese (II) acetate as catalyst dissolved in 2.5mL of water is feeding from a weeping funnel for 1 h. At this level, the reaction mixture is maintained for another 4 h, under vigorous continuous stirring. This time is collected ~4mL of water. Finally, the reaction flask is cooled at room temperature. The magnetic composite is separated by settling, washed by three times with methanol. Then, it is filtered and dried in a vacuum oven at 50°C.

Methods of investigation

The thermal properties of the samples were evaluated using a STA 449 F1 Jupiter apparatus (Netzsch-Germany) in nitrogen atmosphere, with heating rate of $10^oC \cdot min^{-1}$. The samples up to 10 mg weight were placed in Al_2O_3 crucibles and heated between 30-600°C. Friedman (FR) method was applied to calculate the dependence of *E*a on the conversion degree. Based on the *E*a values of thermal degradation processes and the curves shape *E*a *versus* conversion degree (calculated with FR method) and the DTG curves, it is possible to settle if the thermal degradation occurs in one or more stages. Based on these data, kinetic and statistics parameters of the thermal decomposition have been calculated using the multiple non-linear regression method with the "Thermokinetics-3" software.[19] The thermal characterization of the samples was done using a thermobalance STA 449 F1 Jupiter. In Table 3 the studied samples and their notation are presented. Also, the thermal parameters extracted from TG/DTG curves, such as: T_{10} and T_{20} - representing the temperature corresponding to 10 and 20 % mass loss, T_{onset} – the temperature at which the thermal degradation starts, T_{peak} - the temperature at which the degradation rate is maximum and W_f - the final residue mass, are included.

Table 3

The thermal parameters and contact angle values of PSI-b-PEG polymer shell, and also the thermal characteristics of the magnetic composite

Sample	Notation	Degradation stage	T_{onset} °C	T_{peak} °C	W_f %	T_{10} °C	T_{20} °C	Contact angle (°)
								Water
PSI-b-$PEG_{2.000}$	P2	I II III residue	40 275 357	- 327 416	9.76 20.04 32.62 37.58	277	324	43
PSI-b-$PEG_{2.000}$ and 10% magnetite	MC2	I II III residue	35 157 325	64 234 364	4.60 19.38 16.02 60.00	223	307	-
PSI-b-PEG_{4000}	P4	I II III IV residue	40 282 380 482	226 339 423 523	13.48 14.90 22.68 11.26 37.68	234	325	38

Table 3 (continued)

PSI-b-$PEG_{4.000}$ and 10% magnetite	MC4	I II III residue	35 130 315	60 248 360	4.28 16.42 32.13 47.17	219	291	-
PSI-b-$PEG_{10.000}$	P10	I II III residue	115 317 448	218 355 518	15.80 43.90 7.80 32.50	245	328	35
PSI-b-$PEG_{10.000}$ and 10% magnetite	MC10	I II III residue	35 145 302	65 248 367	4.40 44.20 10.40 41.00	232	290	-
PSI-co-$PEG_{20.000}$	P20	I II III residue	112 318 456	220 356 518	4.90 14.05 42.40 38.65	238	324	28
PSI-co-$PEG_{20.000}$ and 10% magnetite	MC20	I II III residue	35 150 305	62 252 371	5.27 14.33 43.40 37.00	217	292	-
10 K/min, N_2, Al_2O_3, 30-600 K								

Contact angle of the block-copolymer surface. All contact angles were measured at ambient conditions (~ 22°C; 30 to 40% rel. humidity) using ultrapure water (ASTM type I water, 18.2MΩ•cm). The static contact angle of the films was determined by the sessile drop method, within 10 s, after placing 1 μL drop of water on the film surface from the polymeric shell (PSI-b-PEG), using a CAM-200 instrument from KSV-Finland. Contact angle was measured at least 10 times on different sites of surface, the average value being considered.

***AFM investigations*.** The film analysis was performed in air at room temperature, in the Tapping Mode using a Scanning Probe Microscope (Solver PRO-M, NTMDT, Russia) with commercially available NSG10/Au Silicon cantilevers. The manufacturer's value for the probe tip radius was 10 nm, and the typical force constant of 11.5 N/m. The cantilever was oscillated close to the resonance frequency (254.249 kHz) over the area to be scanned (20 μm x 20 μm, 30 μm x 30 μm, 40 μm x 40 μm, 60 μm x 60 μm). The scans were done without any sample surface treatment. The films were obtained by the spin-coating method, with a Spin 3000 device and Spin Processor WS-650 series, Laurell Technologies, North Wales.

CONCLUSIONS

In this investigation the deep thermal characterization of the core-shell magnetic composite in relation with the properties of the shell formed from poly(succinimide-b-ethyleneglycol)(PSI-b-PEG), respectively the molecular weight of poly(ethylene glycol), is presented.

The study confirms the dependence of the thermal stability, for both the synthesized block copolymers and the prepared magnetic composites, on the molecular weight of PEG. Also, the influence of the Fe atoms presence was concretized in an autocatalytic effect for thermal degradation. Information resulted from the thermal analysis are sustained by the contact angle values of the block copolymer as well by the morphological aspects of the block copolymer films.

Acknowledgements: This work was financially supported by the grant of the Romanian National Authority for Scientific Research, CNCS-UEFISCDI, project number PN-II-132/2014 Magnetic biomimetic supports as alternative strategy for bone tissue engineering and repair'' (MAGBIOTISS). The authors thank NETZSCH-Gerätebau GmbH for the thermal analyses of the studied samples. The authors appreciate the colleagues Dr. Iuliana Stoica and Dr. Elena Stoleru in "P. Poni" Institute of Macromolecular Chemistry for their expert assistance in AFM and contact angle analyses.

REFERENCES

1. L. E van Vlerken, T. K Vyas and M. M Amiji, *Pharmaceutical Research*, **2007**, *24*, 1405-1414.
2. J. D Andrade**,** V. Hlady, S. I Jeon,. *Adv. Chem. Ser.*, **1996**, *248*, 51-59.
3. J. H Lee, H. B Lee and J. D Andrade, *Prog. Polym. Sci.,* **1995**, *20*, 1043-1079.
4. C. G Golander, J. N Herron, K. Lim, P. Claesson, P. Stenius and J. D Andrade, in "Poly(ethylene glycol) chemistry, biotechnical and biomedical applications", J. M Harris (Ed.), Plenum Press, New York, 1992, p. 221-245.
5. K. Holmberg, K. Bergstrom and M. B Stark, in "Poly(ethylene glycol) chemistry, biotechnical and biomedical applications", J. M Harris (Ed.), Plenum Press, New York, 1992, p. 303-324.
6. S. Nagaoka and A. Nakao, *Biomaterials,* **1990**, *11*, 119-121.
7. S. Roweton, S. J Huang and G. Swift, *J. Environm. Polym. Degrad.,* **1997,** *5,* 175-181.

8. D. D Alford, A. P Wheeler and C. A Pettigrew, *J. Environ. Polym. Degrad.,* **1994**, *2*, 225-236.
9. M. R Freedman, Y. H Paik, G. Swift, R. Wilczynski, S. K Wolk and K. M, *Polym. Repr.,* **1994**, *35*, 423-435.
10. T. Nakato, M. Toshitake, K. Matsubara, M. Tomida and T. Kakuchi, *Macromolecules,* **1998**, *31*, 2107-2116.
11. G. Swift, M. B Freeman, Y. H Paik, E. Simon, S. K Wolk and K. M Yocom, *Macromol. Symp.,* **1997**, *123*, 195-203.
12. A. P Chiriac, L. E Nita and I. Neamtu, *Polimery*, **2010**, *55(9)*, 641-645.
13. A. P Chiriac, L. E Nita, I. Neamtu and V. Badescu, *Appl. Surf. Sci.*, **2010**, *257*, 997-1001.
14. A. P Chiriac, I. Neamtu, L. E Nita and M.T Nistor, *Composites Part B: Engineering*, **2011**, *42*, 1525-1531.
15. K. Knop, R. Hoogenboom, D. Fischer and U. S Schubert, *Angew. Chem. Int.,* **2010**, *49*, 6288-6308.
16. A. V Kabanov, V. P Chekhonin, V. Y Alakhov, E. V Batrakova, A. S Lebedev, N. S Melik-Nubarov, S. A Arzhakov, A. V Levashov and G.V Morozov, *FEBS Lett*, **1989**, *258,* 343-345.
17. G. S Kwon and K. Kataoka, *Adv. Drug Delivery Rev.*, **1995**, *16*, 295-309.
18. S. Svenson and D. A Tomalia, *Adv. Drug Delivery Rev.*, **2005**, *57*, 2106-2129.
19. Netzsch Thermokinetics-3, version 2008.05.
20. J. Opfermann, *J. Therm. Anal. Calorim.,* **2000**, *60*, 641-658.
21. D. Rosu, N. Tudorachi and L. Rosu, *J. Anal. Appl. Pyrol.*, **2010**, *89*, 152-158.
22. P. Kim, D. H Kim, B. Kim, S. K Choi, S. H Lee, A. Khademhosseini, R. Langer and K. Y Suh, *Nanotechnology*, **2005**, *16,* 2420-2426.
23. G. M Harbers, K. Emoto, C. Greef, S. W Metzger, H. N Woodward, J. J Mascali, D. W Grainger, and M. J Lochhead, *Chem. Mater.,* **2007**, *19*, 4405-4414.
24. J. Milton Harris (Ed.), "*Poly(ethylene glycol) chemistry biotechnical and biomedical applications*", Springer Science-Business Media New York, Originally published by Plenum Publishing Corporation, 1992.